ACS APPLIED MATERIALS & INTERFACES

Research Article

www.acsami.org

# Composite Pillars with a Tunable Interface for Adhesion to Rough Substrates

Sarah C. L. Fischer,[†,‡] Eduard Arzt,[†,‡] and René Hensel*[,†]

[†]INM—Leibniz Institute for New Materials, Campus D2 2, 66123 Saarbrücken, Germany

[‡]Department of Materials Science and Engineering, Saarland University, Campus D2 2, 66123 Saarbrücken, Germany

Supporting Information

**ABSTRACT:** The benefits of synthetic fibrillar dry adhesives for temporary and reversible attachment to hard objects with smooth surfaces have been successfully demonstrated in previous studies. However, surface roughness induces a dramatic reduction in pull-off stresses and necessarily requires revised design concepts. Toward this aim, we introduce cylindrical two-phase single pillars, which are composed of a mechanically stiff stalk and a soft tip layer. Adhesion to smooth and rough substrates is shown to exceed that of conventional pillar structures. The adhesion characteristics can be tuned by varying the thickness of the soft tip layer, the ratio of the Young's moduli and the curvature of the interface between the two phases. For rough substrates, adhesion values similar to those obtained on smooth substrates were achieved. Our concept of composite pillars overcomes current practical limitations caused by surface roughness and opens up fields of application where roughness is omnipresent.

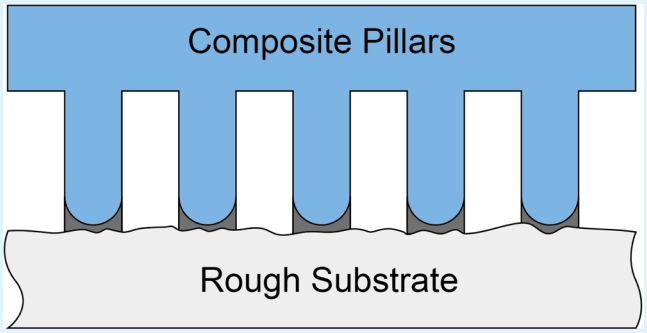


**KEYWORDS:** *dry adhesives, composites, roughness, tunable adhesion, fibrillar, interface curvature*

## 1. INTRODUCTION

Fibrillar dry adhesives attract much attention as they are instrumental for emerging technologies such as wall climbing robots[1] and novel gripping systems.[2,3] In such applications, most real walls and objects exhibit surface roughness on different length scales. It is known that roughness strongly affects adhesion and, for example, limits the maximum lifting force.[4] Several studies were performed which examine the influence of surface roughness on adhesion as a function of the real contact area and elastic material properties.[5−7] An increase in roughness typically leads to a significant loss in contact area and larger distances over which the short-range intermolecular forces have to act. In addition, higher elastic strains typically occur in the contact zone, which also counteract adhesion. In order to improve adhesion, higher preloads and, in the case of viscoelastic materials, longer times in contact with the substrate can help as they tend to enlarge the contact area.[7,8]

An alternative approach to enhance adhesion to rough substrates are fibrillar adhesives.[9−13] Such structures are now well-known from sticky footpads found in nature:[14,15] The fibrillar structures of adhesive organs, developed during evolution for instance in geckoes, make up soft and compliant surfaces which allow easy adaption to roughness at the expense of little strain energy.[16−19] The toe pads exhibit several hierarchical levels, with a stalk splicing into successively finer fibrils and, finally, spatula terminal elements.[20] Several groups have mimicked such hierarchically assembled structures in artificial designs,[21−24] but many unsolved questions remain: introduction of hierarchy, for example, generally reduces the available contact area in synthetic adhesives and increases the propensity to elastic buckling.[25,26]

The ladybug provides another blueprint for the design of fibrillar adhesives.[27] In contrast to the gecko, its adhesive pad consists of cuticular fibrils without hierarchy, but each fibril possesses an axial gradient of Young's modulus. Experiments using nanoindentation have demonstrated that the Young's modulus decreases by 3 orders of magnitude from the stalk to the tip.[27] A numerical study revealed that such a material gradient can also prevent clustering of an array of fibrils, especially for fibrils with high aspect ratio coming into contact with rough substrates.[28] Similar effects were observed in smooth adhesive pads of other insects.[29] Recently, first experimental and numerical studies have been performed for fibrils with axial variations of the Young's modulus adhering to smooth surfaces.[30] It was found that very thin soft tip layers promise the best adhesion enhancements for smooth substrates. Interestingly, Bae et al. demonstrated that a soft tip coating added to a micropatterned fibrillar array improved adhesion to skin, i.e. a compliant and rough surface.[31] However, the underlying adhesion mechanism of composite fibrils on rough substrates is only poorly understood.

**Received:** September 13, 2016
**Accepted:** December 6, 2016
**Published:** December 20, 2016

  

DOI: 10.1021/acsami.6b11642
*ACS Appl. Mater. Interfaces* 2017, 9, 1036−1044

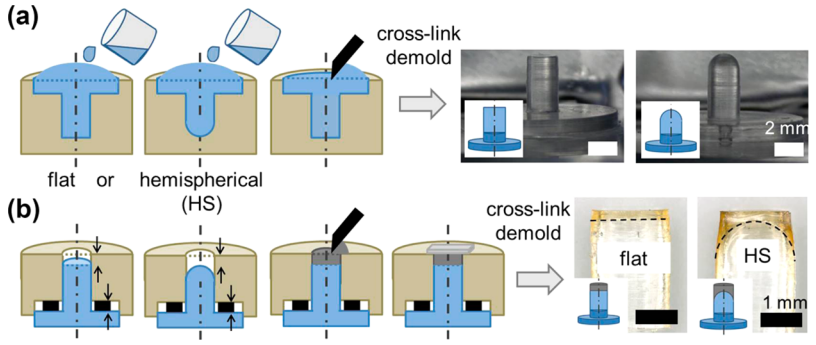


**Figure 1.** Two-step molding process for composite pillar fabrication. (a) Stalks are manufactured in two separate molds depending on the interface geometry of the final composite. The optical micrographs show exemplary PDMS stalks with a flat (left) and a hemispherical (right) pillar face. (b) Adding of soft polyurethane tip layers using a second mold. The thickness of the soft layer is determined by spacers (black) between the mold and the backing layer. Optical micrographs show cross sections of the final composite structures for both interface geometries.

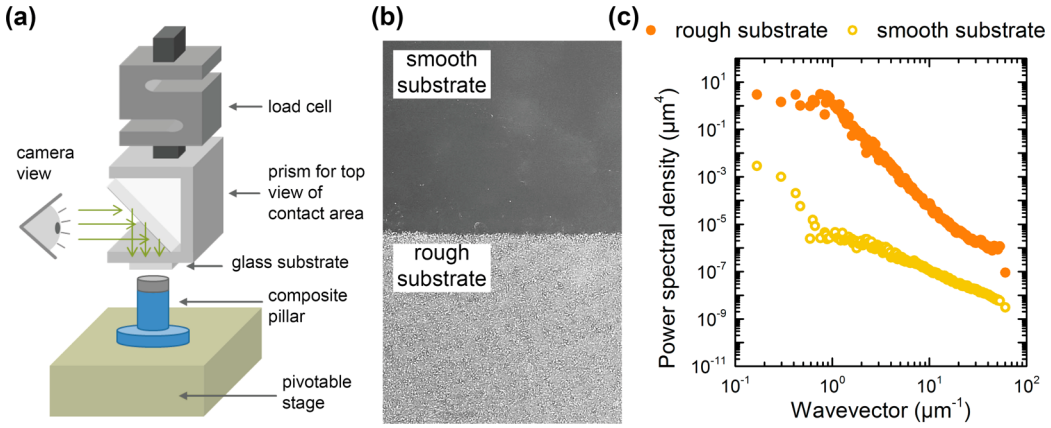


**Figure 2.** Experimental setup for adhesion measurements on smooth and rough substrates. (a) Adhesion measurement setup that consists of a load cell to record normal forces, a pivotable stage for alignment and sample manipulation, and an optical camera for in situ observations of the contact area. (b) The glass slide substrate exhibits two regions: "smooth" and "rough". (c) Corresponding power spectra calculated from AFM data using Surface Topography Analyzer (http://contact.engineering/).[33]

The objective of this work is to evaluate the potential of composite fibrils as a new design concept for adhesion to rough and smooth substrates. As model structures, single macroscopic composite pillars were fabricated in a two-step molding process with a systematic variation of soft layer thickness, Young's modulus ratio, and interface curvature. The influence of these design parameters on adhesion performance and observed detachment events was assessed experimentally. As a result, composite pillars with hemispherical interface, thin soft tips and high Young's modulus ratio were identified as promising candidates to enhance adhesion to rough substrates.

## 2. MATERIAL AND METHODS

**2.1. Fabrication of Composite Pillars.** Composite pillars with macroscopic dimensions in the mm range were fabricated using a two-step molding process as illustrated in Figure 1. The pillars consisted of a relatively stiff stalk of poly(ethylene glycol) dimethacrylate (PEGdma, Polysciences, Warrington, PA, USA; Young's modulus of about 350 MPa) or polydimethylsiloxane (PDMS, Sylgard 184, Dow Corning, Midland, MI, USA; Young's modulus of about 2 MPa). The softer tip layer consisted of polyurethane Polyguss 74-41 (PU, PolyConForm GmbH, Duesseldorf, Germany) with a Young's modulus of about 900 kPa. Thus, composite pillar structures with a Young's modulus ratio of stiff to soft of about 350 and 2, and two interface geometries, flat and hemispherical (with a curvature radius half the diameter), were generated. As control samples, pillars consisting entirely of PU were manufactured.

In the first step of composite fabrication, stalks were replicated using a custom-made aluminum mold as shown in the optical micrograph in Figure 1a. The resulting stalks had a diameter of 2 mm, a height of 4 mm, and either a flat or a hemispherically shaped face with radius 1 mm. The manufacturing process varied for the two materials. The PDMS prepolymer (10 weight parts of the base to 1 weight part of the curing agent) was degassed under vacuum for 5 min at 2000 rpm in a SpeedMixer (DAC600.2 VAC-P, Hauschild Engineering, Hamm, Germany). It was then filled into the mold, degassed for 10 min, and cured at 125 °C for 20 min on a heating plate. In the case of PEGdma, 0.5 wt % of the photoinitiator 2-hydroxy-2-methyl-propiophenone (Sigma-Aldrich, St. Louis, MO, USA) was added to the prepolymer. Subsequently, 1 wt % of 2-aminoethyl methacrylate hydrochloride (Sigma-Aldrich, St. Louis, MO, USA) was added to enhance the adhesion of PU on PEGdma. The liquid mixture was poured into the mold, exposed to nitrogen for 20 min, and then UV-cured for 300 s using a UV lamp (Omnicure S1500, Excelitas Technologies, Waltham, MA, USA).

The soft layer was added to the pillar in the second molding step (Figure 1b): The PU prepolymer solution was mixed under vacuum for 2 min at 2000 rpm in a SpeedMixer. The PDMS stalks required activation with oxygen plasma for 2 min at 60% power (PICO plasma system, Diener electronic, Ebhausen, Germany) prior to this second step to enable covalent bonding of PU to the PDMS. The PU prepolymer was applied at the free end of the pillars and degassed for 2 min. Afterward the excess polymer was removed with a razor blade and the mold was subsequently covered with a smooth Teflon film glued onto a glass slide. To realize different thicknesses of the soft tip, spacers with different thickness were inserted at the back end. The PU


DOI: 10.1021/acsami.6b11642
ACS Appl. Mater. Interfaces 2017, 9, 1036−1044

was cured at room temperature for at least 16 h and finally gently demolded.

**2.2. Adhesion Experiments.** Adhesion experiments were performed using a custom-built, slightly modified setup (Figure 2a) following the work of Kroner et al.[32] A nominally flat glass substrate cut from a soda lime glass microscope slide (Marienfeld, Lauda-Königshofen, Germany) was used as a probe. The glass substrate exhibited two differently rough areas both of which were used for the adhesion tests (Figure 2b): region 1 (designated as "smooth") exhibited a mean absolute roughness $R_a$ = 0.006 $\mu$m, and a mean peak-to-valley profile roughness $R_z$ = 0.041 $\mu$m, while for region 2 (designated as "rough"), $R_a$ = 0.271 $\mu$m and $R_z$ = 2.174 $\mu$m obtained from surface profilometer measurements (DekTak, Bruker, Billerica, MA, USA). Roughness power spectra (Figure 2c) of both substrate regions were calculated by Surface Topography Analyzer developed by Lars Pastewka (http://contact.engineering/)[33] based on AFM topography scans (JPK instruments AG, Berlin, Germany). Both regions were on the same substrate and were used for testing without changing the initial alignment performed on the smooth region of the substrate.

Normal forces were recorded with a load cell (3 N, Tedea-Huntleigh 1004, Vishay Precision Group, Basingstoke, UK). Before each measurement, the substrate was cleaned with ethanol. A camera and a prism, mounted below the sample, were used to optically align the specimen and the substrate and to observe the contact area between the pillars and the substrate in situ. Upon adhesion measurements, samples were sectioned in axial direction and the thickness of the soft tip layer was measured in an optical microscope (Eclipse LV100ND, Nikon, Alzenau, Germany) with an accuracy of ±10 $\mu$m.

In the adhesion experiments, specimen and substrate were brought together until a maximum force, corresponding to compressive preloads between 30 and 180 mN, was reached. After a hold time ranging from 0 to 120 s, the specimen was withdrawn until it detached from the substrate. The measurements were repeated at two different positions on each of the two substrate regions (smooth and rough). For the PEGdma/PU and PDMS/PU composites, the effective elastic moduli of the pillars varied over 2 orders of magnitude. As a result, the applied force rate in adhesion tests varied dramatically. To keep the force rate similar for all samples, the following test velocities were chosen: For PDMS/PU composites and the PU control pillars, experiments were conducted at 10 $\mu$m/s. For PEGdma/PU composites, experiments were performed at 2 $\mu$m/s. Thus, the force rate was about 10 mN/s and comparable for all tested structures.

For the analysis, the recorded force and displacement values were transformed into nominal stress, $\sigma$, and displacement, $\Delta$. We accounted for the deformation of the setup by a correction of the displacement with the previously measured machine compliance ($C$ = 0.12 $\mu$m/mN). Pull-off stress values were determined from the maximum tensile force, divided by the nominal contact area.

## 3. RESULTS

The macroscopic composite pillars fabricated by the technique described above are shown in Figure 1. Flat and hemispherical (curvature radius about 1 mm) interfaces, with soft PU layers in the range between 20 and 500 $\mu$m, were successfully generated. The actual soft layer thickness, $t$, were determined upon adhesion measurements and showed some variation due to slight material shrinkage during the cross-linking reaction. For PEGdma/PU composites, manufacturing difficulties occurred for tip thicknesses below 120 $\mu$m and, therefore, no measurements were performed for those parameters. As a control structure, conventional pillars with the same dimensions made entirely from PU were used.

In a first step, the adhesion characteristics of conventional pillar structures are reported. Figure 3 shows that their adhesion to the smooth substrate was always higher than to the rough substrate: for small preloads (about 50 mN), the pull-off stress was about 25 kPa for the smooth substrate and about 10 kPa for the rough substrate, corresponding to a ratio of about 2.5. This behavior is in line with a recent study by Barreau et al.[10] Unlike smooth substrates, rough substrates gave significantly higher adhesion after applying higher preloads or after longer hold times (Figure 3). Thus, for high preloads (about 150 mN), the ratio decreased to 1.5 for 0 s hold time and to about 1.2 for 120 s hold time. These findings very likely reflect the viscoelastic nature of PU that produces an increase in contact area by material relaxation over time.

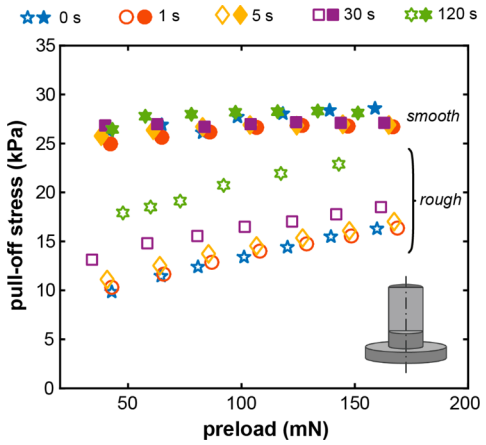


**Figure 3.** Pull-off stress of conventional pillars (controls) made entirely from polyurethane on smooth (filled symbols) and rough substrates (open symbols) as a function of preload and for different hold times: 0 s (blue star), 1 s (red circle), 5 s (yellow diamond), 30 s (purple square), and 120 s (green hexagram).

The pull-off stress of the composite pillars as a function of the soft layer thickness is shown in Figure 4 for two distinct force ranges: low preloads with 50 mN and high preloads with 150 mN. Figure 4a and b illustrate the results for composites with a flat interface: On the smooth substrate, the pull-off stress increased with decreasing soft layer thickness up to a maximum pull-off stress of about 55 kPa (for PDMS/PU composites) and 60 kPa (PEGdma/PU composites); these values are about twice those for the PU control specimen (Figure 4a). The Young's modulus ratio had an influence on the critical thickness, at which the maximum adhesion value was achieved. The critical thickness was about 250 $\mu$m for $E_1/E_2$ = 350 and about 120 $\mu$m for $E_1/E_2$ = 2. With higher preloads, the adhesion of the composites increased slightly (dashed lines). In contrast, the adhesion of the composites with a flat interface on the rough substrate (Figure 4b) was similar to that of the PU control and insensitive to the Young's modulus ratio as well as the soft layer thickness. Only for high preloads (150 mN) was a strong increase in pull-off stress, by a factor of 2, observed. Figures 4c and d illustrate the pull-off stress of the composites with hemispherical interface under small and high preload. On the smooth substrate, adhesion was similar for both preloads whereas it increased with preload for the rough substrate. For both substrates, it was found that the pull-off stress continuously increased with decreasing layer thickness. Particularly for very thin soft layers ($t$ = 30 $\mu$m), the value of about 75 kPa was similar on the smooth and rough substrate and, therefore, much higher than for the PU control sample. Thus, we obtained an increase in pull-off stress, over conventional pillars, of about three times on the smooth substrate (Figure 4c) and about five times on the rough substrate (Figure 4d).


DOI: 10.1021/acsami.6b11642
ACS Appl. Mater. Interfaces 2017, 9, 1036−1044

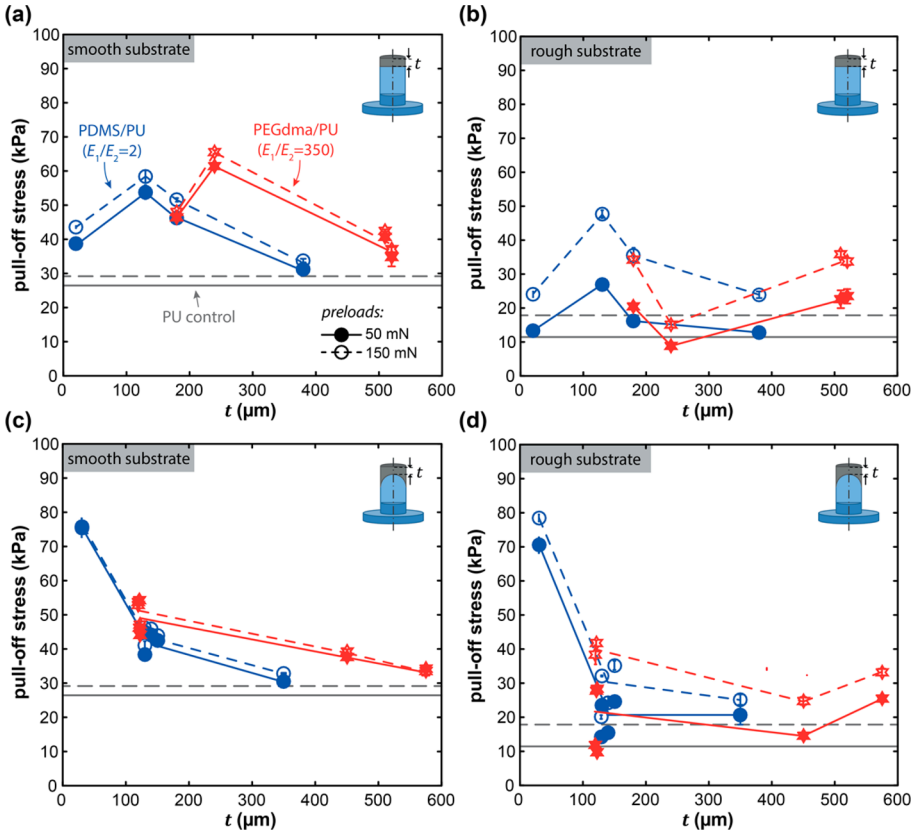


**Figure 4.** Pull-off stress of composite pillars as a function of the soft layer thickness, *t*. Composite pillars made from PDMS/PU (blue circles) and PEGdma/PU (red stars) were tested at different preloads (solid lines and filled symbols for 50 mN, dashed lines and open symbols for 150 mN). The gray horizontal lines represent the pull-off stress of the PU control sample in the low and high preload regime. The time in contact with the substrate was zero seconds. (a, b) Composite structure with flat interface tested on (a) smooth and (b) rough substrate. (c, d) Composite structure with hemispherical interface tested on (c) smooth and (d) rough substrate.

In the adhesion tests, three distinct detachment mechanisms as a function of the soft layer thickness, elastic modulus ratio and interface curvature could be identified (Figure 5):

(i) Edge crack detachment: The crack was initiated at the edge of the pillar and propagated spontaneously through the contact area (Figure 5a). All composite pillars with thick soft layers ($t \geq 250$ $\mu$m for PEGdma/PU and $t \geq 120$ $\mu$m for PDMS/PU), composites with flat interface, $E_1/E_2 = 2$ and thinner soft layers as well as all conventional pillars exhibited this mechanism.

(ii) Fingerlike crack propagation: Several cracks initiated at the edge and slowly propagated toward the center (Figure 5b). Composites with flat interfaces, $E_1/E_2 = 350$ and thinner soft layers displayed this mechanism.

(iii) Center crack delamination: A circular crack initiated at the center of the pillar and slowly propagated toward the edge until fast detachment started upon reaching a critical loss in contact area. The crack covered more than 40% of the original contact area (Figure 5c). Composites with hemispherical interfaces and thinner soft layers displayed this behavior.

Interestingly, edge crack detachment was always spontaneous and resulted in detachment directly upon crack initiation within a few seconds. In contrast, fingerlike and center cracks propagated more slowly; the time for the complete detachment could be controlled by the pulling velocity of the displacement controlled setup and ranged from about 10 to 15 s (at 2 $\mu$m/s) to 2 to 3 s (at 10 $\mu$m/s). The different crack types can be distinguished by inspecting the derivatives of their respective force−displacement curves where crack initiation and propagation corresponds to characteristic drops in stiffness (Figure 5d). The initial stiffness of the pillars correlates with the soft tip layer thickness and is highest for the thinnest tip. Overall, crack initiation resulted in a significant drop in stiffness (see points I, III, and V in Figure 5d) and directly to detachment in case of edge cracks (point II). A less pronounced decrease in stiffness upon crack initiation relates to stable crack propagation driven by further withdrawal of the pillar structure. Unlike edge cracks, the center and finger cracks were not immediately unstable. The transition from edge to finger or center crack with decreasing soft tip thickness was similarly observed on the smooth and the rough substrates.

Similar to conventional pillars (Figure 3), extended hold times yield higher pull-off stress for all composite pillars (Figure 6). The magnitude and rate of increase of the hold time effect were significantly higher for rough substrates and varied with tip layer thickness, the Young's modulus ratio and the interface curvature. Upon contact to the rough substrate, local stresses at the pillar faces induced by surface asperities decreased with time due to viscoelastic material relaxation. In addition, the contact area most likely increased. Hence, reduced local strains and larger contact areas led to higher pull-off stresses as shown in Figure 6. The data obtained from the hold time experiments were fitted using an equation that phenomenologically describes viscoelastic material relaxation. Thus, the pull-off


DOI: 10.1021/acsami.6b11642
ACS Appl. Mater. Interfaces 2017, 9, 1036−1044

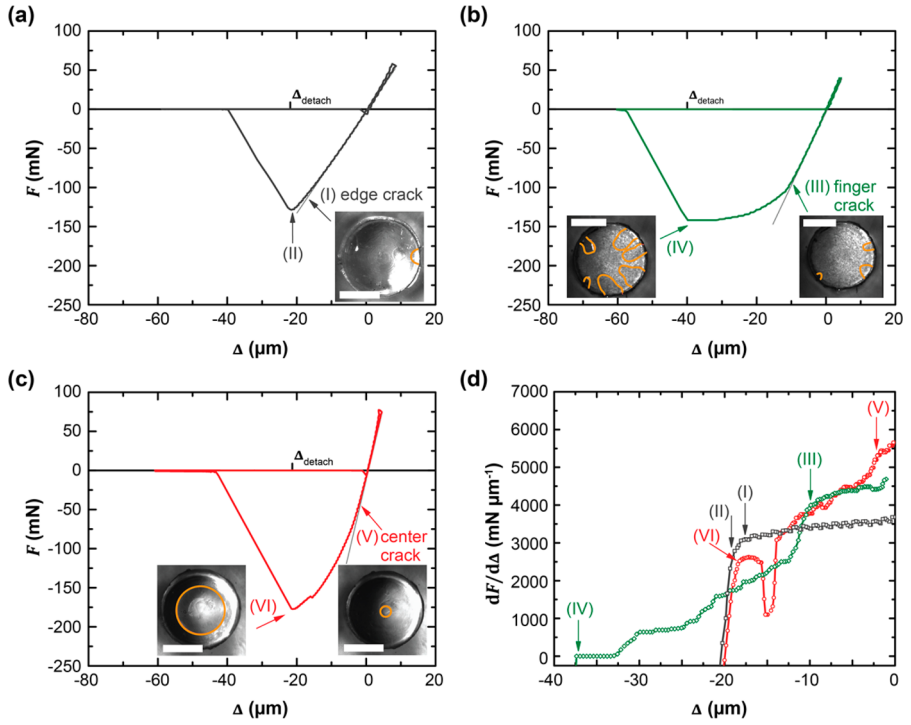


**Figure 5.** Detachment mechanisms of composite pillars. (a–c) Force ($F$) displacement ($\Delta$) curves of PEGdma/PU composite pillars ($E_1/E_2$ = 350) adhered to the smooth substrate. (a) Pillar with hemispherical interface and a 450 $\mu$m thick soft tip: crack initiation (I) spontaneously lead to complete detachment (II) via edge crack. (b) Pillar with flat interface and a 180 $\mu$m tick soft tip: finger cracks (III) appear and grow toward the center (IV) before complete detachment occurs. (c) Pillar with hemispherical interface and a 120 $\mu$m thick soft tip: a center crack (V) is formed and propagate toward the edge (VI) before complete detachment occurs. (d) Derivative of the force–displacement curves in the retracting part of the curves. These represent the decrease in stiffness during crack initiation and propagation. Optical micrographs (insets) visualize the cracks upon initiation and propagation (scale bars: 1 mm). The crack fronts were highlighted with orange lines for better visualization.

stress, $\sigma$, as a function of hold time, $\tau$ can be expressed as follows:

$$\sigma(\tau) = \sigma_\infty - (\sigma_\infty - \sigma_0)\exp\left(-\frac{\tau}{\tau_0}\right) = \sigma_\infty - \Delta\sigma\exp\left(-\frac{\tau}{\tau_0}\right) \quad (1)$$

where $\sigma_0$ is the initial pull-off stress at $\tau$ = 0 s, $\sigma_\infty$ is the maximum pull-off stress for infinite hold times, $\Delta\sigma = \sigma_\infty - \sigma_0$ and $\tau_0$ is the characteristic relaxation time. The fitting parameters were calculated using a nonlinear regression model in Matlab (MathWorks, Ismaning, Germany) based on the Marquardt–Levenberg algorithm.[34,35] All fit parameters can be found in Supporting Information Tables S1 and S2.

For the smooth substrate, the increase in $\Delta\sigma$ was small (2 to 5 kPa) for all samples, signifying that adhesion did not significantly depend on hold time (Figure 6). For the rough substrate, in contrast, longer hold times resulted in higher values of $\Delta\sigma$. Composites with thick soft tip layers, irrespective of interface curvature, exhibited a value of $\Delta\sigma \approx 7$ kPa similar to the value found for the PU control. For thinner tip layers, a strong increase in $\Delta\sigma$ was observed, rising up to 24 kPa for PDMS/PU composites (with hemispherical interface and 30 $\mu$m thick tip) or 32 kPa for PEGdma/PU composites (hemispherical, 120 $\mu$m). Figure 7a displays that $\sigma_\infty/\sigma_0$, i.e. the relative increase in adhesion, was higher for thinner soft layer thickness and higher Young's modulus ratio. For PEGdma/PU composites with hemispherical interface the maximum time-related adhesion ratio was about 6, which is four times higher than for the PU control ($\sigma_\infty/\sigma_0 = 1.6 \pm 0.2$) and the PDMS/PU composites with hemispherical interface ($\sigma_\infty/\sigma_0 = 1.7 \pm 0.3$). For composites with flat interface, the ratio increased from 2 to 4 with smaller tip thickness, but decreased again after a threshold thickness. To assess how fast viscoelastic relaxation occurred, we compared the gradients of $\sigma(\tau)$, i.e. the first derivative of the fit equation (eq 1) at $\tau$ = 0 s, which equals $\Delta\sigma/\tau_0$. Figure 7b shows that the rate is similar or higher, for all composites, when compared to the PU control, suggesting that composite pillars adapt faster to rough substrates. Furthermore, the rate increased with thinner soft tip thickness, but did not vary systematically for the different pillar compositions. The considerable scatter of the values is most likely caused by the strong variation of $\tau_0$ obtained from the fits (see Supporting Information Tables S1 and S2).

## 4. DISCUSSION

The results presented in this paper showed that pull-off forces of composite pillars can significantly exceed the values of conventional pillar structures. The adhesion was found to be affected by interface geometry, material combinations and variations in preload as well as hold time. A particularly significant result was that composite pillars exhibited similar adhesion values to both smooth and rough substrates, while the adhesion dropped by more than 50% for conventional pillars.

In the pull-off experiments, the adhesion of composites to the smooth substrate was increased by reducing the soft tip thickness (Figure 4) in accordance with a similar concept recently presented by Minsky and Turner.[30] In addition, numerical simulations revealed that the stress distribution along the pillar–substrate interface dramatically varied with the soft layer thickness, Young's modulus ratio, and materials interface curvature as shown in Supporting Information Figure S1.


DOI: 10.1021/acsami.6b11642
ACS Appl. Mater. Interfaces 2017, 9, 1036–1044

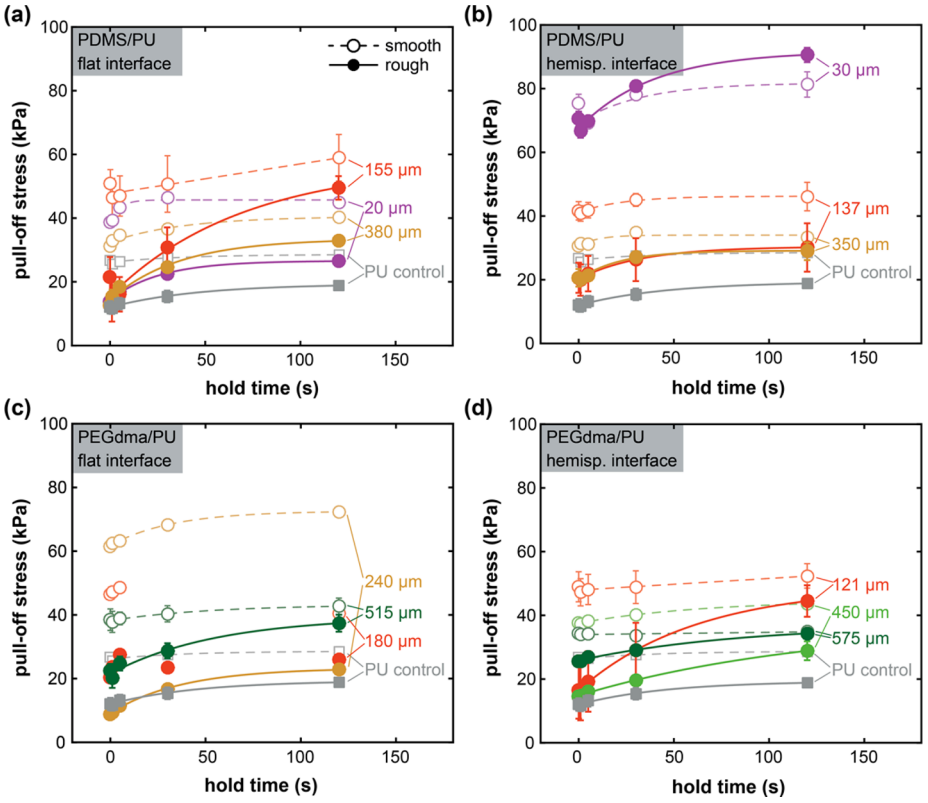


**Figure 6.** Hold time effects on pull-off stress of composite pillars with varying soft layer thickness. (a) PDMS/PU pillar with flat interface. (b) PDMS/PU pillar with hemispherical interface. (c) PEGdma/PU pillar with flat interface. (d) PEGdma/PU pillar with hemispherical interface. The data marked PU control (gray squares) correspond to conventional pillars (cf Figure 3). The adhesion experiments (preload of 50 mN) were performed against smooth (open circle, dashed lines) and rough (filled circle, solid lines) substrates. The solid and dashed lines were fitted using eq 1.

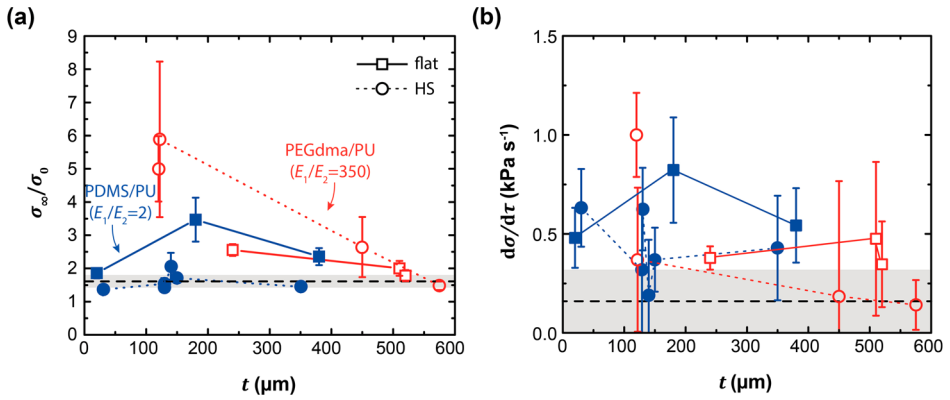


**Figure 7.** Hold time-related relative increase in adhesion $\sigma_\infty/\sigma_0$ and rate of adhesion enhancement $\Delta\sigma/\tau_0$ of composite pillars adhered to rough substrates. (a) Ratio $\sigma_\infty/\sigma_0$ is displayed as a function of the soft tip thickness, $t$. The ratio is calculated from the pull-off stress at infinite hold times, $\sigma_\infty$, divided by the initial pull-off stress, $\sigma_0$ at zero hold time. (b) Rate of adhesion enhancement provides a measure of the time dependent adaptation to the surface topography obtained from the derivative of the fit equation (eq 1) at $\tau = 0$ s and is displayed as a function of the soft tip thickness, $t$. All values for PDMS/PU composite pillars are shown as filled blue and, for PEGdma/PU composite pillars, as open red symbols. Flat interfaces are marked with squares and hemispherical interfaces with circles. The values of the PU control are shown as dashed black lines and their error bars are represented by gray areas.

Particularly, the stresses at the center of the fibril increased with decreasing soft layer thickness, i.e., increasing confinement. Hence, the propensity for edge crack detachment (as always observed for the PU control) decreased and a transition to other crack forms was observed. The distinct crack types depend on the interface geometry and elastic modulus ratio (Figure 5).

For flat interfaces, finger crack detachment with an undulating crack front was initiated close to the perimeter and subsequently propagated toward the center of the contact for high elastic modulus ratio (Figure 5b) and edge crack for the lower elastic modulus ratio. Finger cracks were frequently reported in pull-off tests on confined viscoelastic layers such as pressure sensitive adhesives or other thin soft films.[36,37] It was also demonstrated that fingering instabilities in thin, soft layers


DOI: 10.1021/acsami.6b11642
ACS Appl. Mater. Interfaces 2017, 9, 1036−1044

are caused by the viscoelastic properties of the material.[38−40] Indeed, the shape of the crack front forms such that the compliance of the layer is maximized for the current contact area and displacement.[41] Theoretical arguments are in agreement with the observed transition from edge to finger cracks for thinner soft layers: Webber et al. calculated the energy release rate as a function of the confinement, which is analogous to the ratio of the pillar radius to the tip layer thickness in our study.[41] Based on their results, one can distinguish between spontaneously propagating edge cracks (energy release rate always higher than the critical energy release rate) and controlled crack propagation of finger cracks (energy release rate always lower than the critical energy release rate). The critical value of the confinement for a rigid punch[41] is about 0.45 and, thus, much smaller than our values obtained for the transition, which are about 4 and 7 for the PEGdma/PU and PDMS/PU composites, respectively. We assume that the increase in the critical confinement value is due to the reduced Young's modulus of the stalk materials compared to the rigid glass punch used in the work of Webber et al.

For hemispherical interfaces (and thin soft layers), detachment occurred at the center of the contact under the high stress concentrations there (Supporting Information Figure S1), leading to a circular crack front propagating toward the edge (Figure 5c). Similar detachment mechanisms have been reported for mushroom structures by Micciché et al.[42] and Heepe et al.[43] Also in these studies, the tip geometry modification reduced the propensity for edge cracks induced by corner stress singularities, while a transition to center cracks was induced.[44−46] A more detailed numerical study on the interfacial stress distribution and, in particular, on the intensity of the corner stress singularities as a function of the composite design parameters is currently underway.[47] In addition to the variation of the interfacial stress distribution, reduced pressure inside the cavities upon center crack formation might contribute to the adhesion. However, a pressure difference would require perfect sealing at the contact area to avoid gas flow. On the rough substrate, such a sealing would be difficult to obtain. It is, therefore, very interesting that the adhesion of composite pillars with hemispherical interface and particularly thin tips exceeded the adhesion of composites with flat interfaces and conventional pillars. The higher adhesion probably results from larger contact areas that were most likely induced by the high center stresses under compressive preloads, which translate into high center stresses in tension during detachment. Such stresses are more beneficial than high stresses at the perimeter in case of conventional pillars (or thick tips) due to edge stress intensities.

In addition to interface geometry, the preload and hold time had a significant impact on the adhesion to rough surfaces, which is in accordance with previous reports.[8,48] Higher preloads enforce the conformation of the pillar faces to the asperities of the substrate topography. Longer hold times most likely reduce local stress concentrations at the pillar faces based on material relaxation. The different material combinations revealed that composite pillars with high Young's modulus ratio and thin tips adapted more quickly to rough substrates as expressed by the highest pull-off stress ratio $\sigma_\infty/\sigma_0$. Again, the stress concentration at the center of the contact area most likely enforces the best adaption to the rough substrate in short hold times. These findings have implications for many areas were dry adhesives can be applied, particularly when objects exhibit microscale roughness in conjunction with short cycle times, as is the case, e.g., in pick-and-place technologies.

## 5. CONCLUSION

We presented a detailed study on composite pillars that overcome previous limitations in adhesion to rough glass substrates. For the first time, a systematic variation of structure parameters such as soft tip layer thickness, Young's modulus ratio, and interface geometry was experimentally performed and analyzed in relation to parameters such as surface roughness, preload, and hold time. The following conclusions can be drawn:

- Composite pillars improved adhesion to the smooth and rough substrates by a factor of 3 and 5 compared to conventional pillar structures made from a single material.
- To take advantage of this effect, composite structures should exhibit thin soft tips atop a stiffer stalk. Curved material interfaces were found to be beneficial compared to flat interfaces as high center stresses enforce the adaption to surface asperities and, therefore, result in higher adhesion.
- The edge crack detachment due to sharp corners of the pillars undergoes a transition to center crack (hemispherical interface) or finger crack (flat interface) below a critical tip layer thickness that depends on the Young's modulus ratio.
- Preload and hold time have a strong impact on adhesion of the composite pillars to the rough substrate but affect only slightly the adhesion to the smooth substrate. For the rough substrate, the pull-off stress ratio between infinite and zero seconds hold times as well as the rate to adapt to the surface topography are highest for the composite pillar with hemispherical interface and Young's modulus ratio of 350.

We believe that these results are particularly relevant for the design of fibrillar adhesives suitable for applications in the presence of surface roughness.

## ■ ASSOCIATED CONTENT

### Supporting Information

The Supporting Information is available free of charge on the ACS Publications website at DOI: 10.1021/acsami.6b11642.

List of parameters obtained from fit equation (eq 1) and FE analyses on interfacial stress distributions for different composite pillars (PDF)

## ■ AUTHOR INFORMATION


### Corresponding Author

*Phone: +49 (0)681-9300-390. Fax: +49 (0)681-9300-223. E-mail: rene.hensel@leibniz-inm.de.

### ORCID

René Hensel: 0000-0002-9623-2118


### Author Contributions

All authors contributed to conception and experimental design. S.C.L.F. performed the experiments and simulations and carried out analysis of data. All authors wrote the manuscript.

### Notes

The authors declare no competing financial interest.



DOI: 10.1021/acsami.6b11642
ACS Appl. Mater. Interfaces 2017, 9, 1036−1044

## ■ ACKNOWLEDGMENTS

The authors acknowledge Prof. Robert M. McMeeking (UC Santa Barbara, USA), Prof. Attila Kossa (Budapest University of Technology and Economics, Hungary), and RamGopal Balijepalli for helpful discussions on the contact mechanics of composite pillars. The authors further thank Martin Schmitz, Susanne Selzer, and Lukas Engel for their technical support. S.C.L.F. would like to thank Michael M. Becker (Fraunhofer Institute for Nondestructive Testing, Saarbrücken) for discussions and computing time on the Comsol server. The research leading to these results has received funding from the European Research Council under the European Union's Seventh Framework Programme (FP/2007-2013)/ERC Grant Agreement no. 340929 and by the German Research Foundation (Deutsche Forschungsgemeinschaft) through the grant no. HE 7498/1-1.

## ■ REFERENCES

(1) Yu, J.; Chary, S.; Das, S.; Tamelier, J.; Turner, K. L.; Israelachvili, J. N. Friction and Adhesion of Gecko-Inspired PDMS Flaps on Rough Surfaces. *Langmuir* **2012**, *28* (31), 11527−11534.

(2) Zhou, M.; Tian, Y.; Sameoto, D.; Zhang, X.; Meng, Y.; Wen, S. Controllable Interfacial Adhesion Applied to Transfer Light and Fragile Objects by Using Gecko Inspired Mushroom-Shaped Pillar Surface. *ACS Appl. Mater. Interfaces* **2013**, *5* (20), 10137−10144.

(3) Purtov, J.; Frensemeier, M.; Kroner, E. Switchable Adhesion in Vacuum Using Bio-Inspired Dry Adhesives. *ACS Appl. Mater. Interfaces* **2015**, *7* (43), 24127−24135.

(4) King, D. R.; Bartlett, M. D.; Gilman, C. A.; Irschick, D. J.; Crosby, A. J. Creating Gecko-Like Adhesives for "Real World" Surfaces. *Adv. Mater.* **2014**, *26* (25), 4345−4351.

(5) Fuller, K. N. G.; Tabor, D. The Effect of Surface Roughness on the Adhesion of Elastic Solids. *Proc. R. Soc. London, Ser. A* **1975**, *345* (1642), 327−342.

(6) Pastewka, L.; Robbins, M. O. Contact between Rough Surfaces and a Criterion for Macroscopic Adhesion. *Proc. Natl. Acad. Sci. U. S. A.* **2014**, *111* (9), 3298−3303.

(7) Persson, B. N. J.; Albohr, O.; Creton, C.; Peveri, V. Contact Area between a Viscoelastic Solid and a Hard, Randomly Rough, Substrate. *J. Chem. Phys.* **2004**, *120* (18), 8779−8793.

(8) Creton, C.; Leibler, L. How Does Tack Depend on Time of Contact and Contact Pressure? *J. Polym. Sci., Part B: Polym. Phys.* **1996**, *34* (3), 545−554.

(9) Persson, B. N. J. On the Mechanism of Adhesion in Biological Systems. *J. Chem. Phys.* **2003**, *118* (16), 7614−7621.

(10) Barreau, V.; Hensel, R.; Guimard, N. K.; Ghatak, A.; McMeeking, R. M.; Arzt, E. Fibrillar Elastomeric Micropatterns Create Tunable Adhesion Even to Rough Surfaces. *Adv. Funct. Mater.* **2016**, *26* (26), 4687−4694.

(11) Huber, G.; Gorb, S. N.; Hosoda, N.; Spolenak, R.; Arzt, E. Influence of Surface Roughness on Gecko Adhesion. *Acta Biomater.* **2007**, *3*, 607−610.

(12) Kasem, H.; Varenberg, M. Effect of Counterface Roughness on Adhesion of Mushroom-Shaped Microstructure. *J. R. Soc., Interface* **2013**, *10* (87), 20130620−20130620.

(13) Vajpayee, S.; Jagota, A.; Hui, C.-Y. Adhesion of a Fibrillar Interface on Wet and Rough Surfaces. *J. Adhes.* **2010**, *86* (1), 39−61.

(14) Labonte, D.; Clemente, C. J.; Dittrich, A.; Kuo, C.-Y.; Crosby, A. J.; Irschick, D. J.; Federle, W. Extreme Positive Allometry of Animal Adhesive Pads and the Size Limits of Adhesion-Based Climbing. *Proc. Natl. Acad. Sci. U. S. A.* **2016**, *113* (5), 1297−1302.

(15) Gorb, S.; Gorb, E.; Kastner, V. Scale Effects on the Attachment Pads and Friction Forces in Syrphid Flies (Diptera, Syrphidae). *J. Exp. Biol.* **2001**, *204* (8), 1421−1431.

(16) Arzt, E.; Gorb, S.; Spolenak, R. From Micro to Nano Contacts in Biological Attachment Devices. *Proc. Natl. Acad. Sci. U. S. A.* **2003**, *100* (19), 10603−10606.

(17) Zhou, M.; Pesika, N.; Zeng, H.; Tian, Y.; Israelachvili, J. Recent Advances in Gecko Adhesion and Friction Mechanisms and Development of Gecko-Inspired Dry Adhesive Surfaces. *Friction* **2013**, *1* (2), 114−129.

(18) Kamperman, M.; Kroner, E.; del Campo, A.; McMeeking, R. M.; Arzt, E. Functional Adhesive Surfaces with "Gecko" Effect: The Concept of Contact Splitting. *Adv. Eng. Mater.* **2010**, *12* (5), 335−348.

(19) Heepe, L.; Gorb, S. N. Biologically Inspired Mushroom-Shaped Adhesive Microstructures. *Annu. Rev. Mater. Res.* **2014**, *44* (1), 173−203.

(20) Autumn, K.; Gravish, N. Gecko Adhesion: Evolutionary Nanotechnology. *Philos. Trans. R. Soc., A* **2008**, *366* (1870), 1575−1590.

(21) Kim, S.; Sitti, M. Biologically Inspired Polymer Microfibers with Spatulate Tips as Repeatable Fibrillar Adhesives. *Appl. Phys. Lett.* **2006**, *89* (26), 261911.

(22) Greiner, C.; Del Campo, A.; Arzt, E. Adhesion of Bioinspired Micropatterned Surfaces: Effects of Pillar Radius, Aspect Ratio, and Preload. *Langmuir* **2007**, *23*, 3495−3502.

(23) Hui, C.-Y.; Jagota, A.; Shen, L.; Rajan, A.; Glassmaker, N.; Tang, T. Design of Bio-Inspired Fibrillar Interfaces for Contact and Adhesion — Theory and Experiments. *J. Adhes. Sci. Technol.* **2007**, *21*, 1259−1280.

(24) Gorb, S. N.; Varenberg, M. Mushroom-Shaped Geometry of Contact Elements in Biological Adhesive Systems. *J. Adhes. Sci. Technol.* **2007**, *21* (12−13), 1175−1183.

(25) Spolenak, R.; Gorb, S.; Arzt, E. Adhesion Design Maps for Bio-Inspired Attachment Systems. *Acta Biomater.* **2005**, *1* (1), 5−13.

(26) Bauer, C. T.; Kroner, E.; Fleck, N. A.; Arzt, E. Hierarchical Macroscopic Fibrillar Adhesives: In Situ Study of Buckling and Adhesion Mechanisms on Wavy Substrates. *Bioinspiration Biomimetics* **2015**, *10* (6), 66002.

(27) Peisker, H.; Michels, J.; Gorb, S. N. Evidence for a Material Gradient in the Adhesive Tarsal Setae of the Ladybird Beetle Coccinella Septempunctata. *Nat. Commun.* **2013**, *4*, 1661.

(28) Gorb, S. N.; Filippov, A. E. Fibrillar Adhesion with No Clusterisation: Functional Significance of Material Gradient along Adhesive Setae of Insects. *Beilstein J. Nanotechnol.* **2014**, *5* (1), 837−845.

(29) Scholz, I.; Baumgartner, W.; Federle, W. Micromechanics of Smooth Adhesive Organs in Stick Insects: Pads Are Mechanically Anisotropic and Softer towards the Adhesive Surface. *J. Comp. Physiol., A* **2008**, *194* (4), 373−384.

(30) Minsky, H. K.; Turner, K. T. Achieving Enhanced and Tunable Adhesion via Composite Posts. *Appl. Phys. Lett.* **2015**, *106* (20), 201604.

(31) Bae, W. G.; Kim, D.; Kwak, M. K.; Ha, L.; Kang, S. M.; Suh, K. Y. Enhanced Skin Adhesive Patch with Modulus-Tunable Composite Micropillars. *Adv. Healthcare Mater.* **2013**, *2* (1), 109−113.

(32) Kroner, E.; Blau, J.; Arzt, E. Note: An Adhesion Measurement Setup for Bioinspired Fibrillar Surfaces Using Flat Probes. *Rev. Sci. Instrum.* **2012**, *83* (1), 16101.

(33) Jacobs, T.; Junge, T.; Pastewka, L. Quantitative Characterization of Surface Topography Using Spectral Analysis. *arXiv* **2016**, *1607*, 03040.

(34) Marquardt, D. W. An Algorithm for Least-Squares Estimation of Nonlinear Parameters. *J. Soc. Ind. Appl. Math.* **1963**, *11* (2), 431−441.

(35) More, J. J. The Levenberg-Marquardt Algorithm: Implementation and Theory. In *Numerical Analysis*; Watson, G. A., Ed.; Lecture Notes in Mathematics; Springer: Berlin Heidelberg, 1978; Vol. *630*, pp 105−116.

(36) Creton, C.; Lakrout, H. Micromechanics of Flat-Probe Adhesion Tests of Soft Viscoelastic Polymer Films. *J. Polym. Sci., Part B: Polym. Phys.* **2000**, *38* (7), 965−979.

(37) Nase, J.; Lindner, A.; Creton, C. Pattern Formation during Deformation of a Confined Viscoelastic Layer: From a Viscous Liquid to a Soft Elastic Solid. *Phys. Rev. Lett.* **2008**, *101* (7), 74503.



DOI: 10.1021/acsami.6b11642
*ACS Appl. Mater. Interfaces* 2017, 9, 1036−1044

(38) Ghatak, A.; Chaudhury, M. K.; Shenoy, V.; Sharma, A. Meniscus Instability in a Thin Elastic Film. *Phys. Rev. Lett.* **2000**, *85* (20), 4329−4332.
(39) Shull, K. R.; Flanigan, C. M.; Crosby, A. J. Fingering Instabilities of Confined Elastic Layers in Tension. *Phys. Rev. Lett.* **2000**, *84* (14), 3057−3060.
(40) Mönch, W.; Herminghaus, S. Elastic Instability of Rubber Films between Solid Bodies. *Europhys. Lett.* **2001**, *53* (4), 525−531.
(41) Webber, R. E.; Shull, K. R.; Roos, A.; Creton, C. Effects of Geometric Confinement on the Adhesive Debonding of Soft Elastic Solids. *Phys. Rev. E: Stat. Phys., Plasmas, Fluids, Relat. Interdiscip. Top.* **2003**, *68* (2), 21805.
(42) Micciché, M.; Arzt, E.; Kroner, E. Single Macroscopic Pillars as Model System for Bioinspired Adhesives: Influence of Tip Dimension, Aspect Ratio, and Tilt Angle. *ACS Appl. Mater. Interfaces* **2014**, *6* (10), 7076−7083.
(43) Heepe, L.; Kovalev, A. E.; Filippov, A. E.; Gorb, S. N. Adhesion Failure at 180 000 Frames per Second: Direct Observation of the Detachment Process of a Mushroom-Shaped Adhesive. *Phys. Rev. Lett.* **2013**, DOI: 10.1103/PhysRevLett.111.104301.
(44) Akisanya, A. R.; Fleck, N. A. Interfacial Cracking from the Freeedge of a Long Bi-Material Strip. *Int. J. Solids Struct.* **1997**, *34* (13), 1645−1665.
(45) Khaderi, S. N.; Fleck, N. A.; Arzt, E.; McMeeking, R. M. Detachment of an Adhered Micropillar from a Dissimilar Substrate. *J. Mech. Phys. Solids* **2015**, *75*, 159−183.
(46) Balijepalli, R. G.; Begley, M. R.; Fleck, N. A.; McMeeking, R. M.; Arzt, E. Numerical Simulation of the Edge Stress Singularity and the Adhesion Strength for Compliant Mushroom Fibrils Adhered to Rigid Substrates. *Int. J. Solids Struct.* **2016**, *85−86*, 160−171.
(47) Balijepalli, R.; Fischer, S. C. L.; Hensel, R.; McMeeking, R. M.; Arzt, E. Numerical Study of Adhesion Enhancement by Composite Fibrils with Soft Tip Layers. *J. Mech. Phys. Solids* **2016**, DOI: 10.1016/j.jmps.2016.11.017.
(48) Persson, B. N. J.; Scaraggi, M. Theory of Adhesion: Role of Surface Roughness. *J. Chem. Phys.* **2014**, *141* (12), 124701.


DOI: 10.1021/acsami.6b11642
*ACS Appl. Mater. Interfaces* 2017, 9, 1036−1044